Building and Environment 98 (2016) 71–79

Contents lists available at ScienceDirect

Building and Environment

journal homepage: www.elsevier.com/locate/buildenv

Predicting single-sided airflow rates based on primary school experimental study

Yuqiao Tang [a,*], Xiaofeng Li [a], Wumengjian Zhu [b], Pok Lun Cheng [a]

[a] Department of Building Science, Tsinghua University, Beijing 100084, China
[b] School of Architecture, Tsinghua University, Beijing 100084, China

ARTICLE INFO

Article history:
Received 5 October 2015
Received in revised form
26 December 2015
Accepted 29 December 2015
Available online 2 January 2016

Keywords:
Airflow rate
Full-scale experiment
Natural ventilation
Single-sided
Thermal buoyancy
Window opening

ABSTRACT

Primary schools in Chinese cities are predominantly located in high-density urban environments with the majority of these schools lacking air conditioning systems. They are extremely dependent on buoyancy-driven natural ventilation because of their location in dense neighborhoods, where local wind velocity is low. This dependency is especially relevant in summer and season transitions, when the temperature difference is small and the relative wind velocity is close to zero. The current authors conducted 168 h of experiments that measured airflow rates in a primary school located in a high-density neighborhood in Beijing. Results from the experiments were used to verify existing correlations that predict airflow rates using meteorological parameters. Three out of the four existing correlations presented a satisfactory prediction when $\Delta T \geq 1$ °C. However, when $\Delta T < 1$ °C, no correlation presented a usable prediction. Therefore, this paper proposes a new hypothetical correlation to predict airflow rates that can accommodate ranges for all temperature differences.

1. Introduction

Indoor air quality in primary schools is an ongoing concern for students and their families. Numerous studies have shown that building occupants in poor indoor air quality are more vulnerable to Sick Building Syndrome (SBS) [1]. Numerous researchers have demonstrated that natural ventilation is an effective way to achieve high indoor air quality and thermal comfort [2–4] which makes the study of natural ventilation in primary schools a popular topic [5,6].

Turanjanin et al. (2014) measured CO_2 concentrations in five schools using the decay method during a hot season in Serbia. The results showed that classrooms in Serbian schools had inadequate ventilation, with CO_2 concentration often exceeding 1000 ppm. These levels can cause health problems for students, thereby increasing their absence from school [7]. In 2004, a team led by D. G. Shendell discovered that a 1000 ppm increase in dCO_2 (indoor minus outdoor carbon dioxide concentration) was associated ($P < 0.05$) with a 0.5–0.9% decrease in annual average daily attendance, corresponding to a relative 10–20% increase in student absences [8].

Compared with office buildings, primary school classrooms are designed with a minimum area of 1.10 m^2 per capita. This area is only one third that of an office building (3 m^2), which subjects primary school students to higher risks [9,10]. As such, a major question to be answered is whether natural ventilation alone can meet the fresh air needs of primary school classrooms. Previous research conducted in the United States of America (US) and Denmark suggests that ventilation rates in primary schools are likely to be below the ASHRAE advised 8 L/s-person. Also, approximately half of the schools in the US, Canada, and Europe were reported to have an average CO_2 concentration measuring above 1000 ppm [6,7].

In China, You et al. (2007) conducted a series of experiments at Nankai University, Tianjin. The team measured ventilation conditions and low air quality related symptoms in 50 rooms, including classrooms, conference rooms, and dormitories. More complaints and symptoms were found in rooms where air exchange rates (AER) were lowest [11]. However, at present, specific data for Chinese primary schools are not readily available, which leaves further research to be done in this area.

Although natural ventilation has limitations that include ventilation heat loss and selective application in specific climates (such as cold winters) [12], government funded primary schools in China are generally not equipped with air conditioning systems

* Corresponding author.
E-mail address: tang_yq@qq.com (Y. Tang).

http://dx.doi.org/10.1016/j.buildenv.2015.12.021
0360-1323/

[10]. Relevant considerations here include the ongoing financial burden of air conditioner installation and maintenance, as well as the risk that these systems pose to spreading air-related epidemics. As a result, for summer and season transitions, natural ventilation plays a key role in maintaining the indoor air quality of primary school classrooms in China.

Based on meteorological records measured at Tsinghua University (Beijing) in summer and season transitions (Mar. to Nov.) from 2010 to 2014, static wind comprised approximately 50% of the wind patterns with a wind speed of less than 0.5 m/s at 10 m above ground level. According to Chinese building codes, the height of a primary school building is limited to four stories (approximately 15 m). Also, for health and safety reasons, all classrooms are required to have doors and windows that have direct access to the outdoor environment [10].

In general, tier one cities in China, such as Beijing, contain urban environments filled with high-rise towers and other multi-story buildings. Typically, this produces low wind speeds in the vicinity of low-rise building windows. Therefore, research on building ventilation with low wind speed and pressure is crucial. Furthermore, the importance of this research also extends to circumstances where thermal pressure is low (such as Beijing) and where temperature differences between the indoor and outdoor environment (in summer and season transitions) result in low thermal pressure.

The experiments for the current research were conducted in a newly built primary school in downtown Beijing. The school is a typical Chinese primary school with no air conditioning, but with doors and windows opened to a semi-outdoor atrium. These conditions ensured that the sample building was in an ideal location for a single-sided ventilation study. The location of the school (highly-dense urban neighborhood) and the time period (March and April) both represented a typical 'worst-case scenario' for Chinese primary schools with regards to air quality control.

Many previous studies focused on certain features of single-sided ventilation, such as driving force [13,14], flow characteristics [15], or single-story building applications [16]. Also, previous simulations focused on predicting airflow rate [17,18], airflow modeling [19,20], and design analysis [21–24]. However, due to limitations of the traditional tracer gas method [25,26], previous theories were seldom tested using large sums of data samples. Therefore, the purpose of this paper is to verify existing correlations for single-sided ventilation with results obtained from full-scale experiments using the tracer gas dry ice method [26]. Then, to use the verifications to determine a suitable correlation that can predict airflow rates in circumstances where thermal pressure and wind velocity are low. This may assist the design of future schools with regards to general and ventilation-specific opening dimensions.

2. Review of existing correlations

Numerous measurements and simulations have previously been undertaken for single-sided natural ventilation that are driven by thermal buoyancy or wind pressure (or both). Several equations have been proposed to solve airflow rates based on temperature and wind velocity parameters.

2.1. The Bernoulli equation

This equation considers the bi-directional airflow occurring through a large, vertical opening between two zones of different temperature. The equation assumes there is a neutral pressure level in the middle of the opening height, $\Delta p(y = H/2) = 0$, a constant temperature in both rooms, and linear pressure profiles (it also applies the ideal gas law); as such, an integration in the vertical direction can be derived to calculate the airflow rate, Q:

$$Q = W \int_{y=0}^{y=H/2} \sqrt{\frac{2\Delta p(y)}{\rho}} \mathrm{d}y \tag{1}$$

where Δp is the pressure difference across the opening (Pa); ρ is the fluid density (kg/m^3); H is the opening height (m); and W is the opening width (m).

This leads to the airflow rate into the room:

$$Q = \frac{1}{3} C_\mathrm{D} A \sqrt{gH \frac{T_\mathrm{i} - T_\mathrm{o}}{T_\mathrm{i}}} \tag{2}$$

where Q is the airflow rate (m^3/s); C_D is the discharge coefficient; A is the area of the opening (m^2); T_i is the internal temperature (K); T_o is the external temperature (K); and g is the gravitational acceleration (m/s^2)

Eq. (2) is often referred to as the Bernoulli equation [17,27].

An empirical constant, C_D, is introduced in Eq. (2) in order to allow for effects such as viscosity, streamline contraction, swirling flow and turbulence. The value of C_D is determined by the characteristics of both the opening shape and the flow field. Usually, C_D is set at 0.6 [20,27,28]. Based on a series of CFD simulations conducted by Favarolo and Manz in 2005, the value of C_D can vary from 0.4 to 0.7 due to wall thickness, number of openings, width of opening, and dimensionless height, (H′) of the opening. H′ is defined as:

$$H' = \frac{d_f}{H_{room} - H} \tag{3}$$

where d_f is the height of the window sill; H_{room} is the height of the room; and H is the height of the opening.

According to CFD simulation results, C_D can be set at 0.6 when H′ is close to 0 and set at 0.7 when H′ is close to 1 [17].

2.2. Correction of Bernoulli equation

In 1995, Dascalaki et al. used a correction factor (CF) to replace the discharge coefficient (C_D):

$$Q = CF \cdot \frac{1}{3} A \sqrt{gH \frac{T_\mathrm{i} - T_\mathrm{o}}{T_\mathrm{i}}} \tag{4}$$

By measuring 52 single-sided natural ventilation configurations using the N_2O tracer gas decay method, they found that CF could be calculated by:

$$CF = 0.08 \left(Gr/Re_D^2\right)^{-0.38} \tag{5}$$

Here, $Gr = \frac{g\Delta TH^3}{T\upsilon^2}$ is the Grashof number;
$Re_D = \frac{UD}{\upsilon}$ is the redefined Reynolds number;
where υ is air viscosity (m^2 s^{-1}) and H and D are the characteristic lengths of the flow (m).

2.3. Combined effect of wind and thermal buoyancy

In most cases, the airflow rate of a building is simultaneously determined by thermal buoyancy, wind pressure and other factors such as air fluctuation. Previous research focused on proposing a correlation that could predict the airflow rate of single-sided ventilation driven by the combination of wind pressure and thermal buoyancy.

In 1982, de Gids and Phaff carried out experiments at three different locations on buildings in urban environments that were surrounded by other buildings up to four floors high. The total number of measurement cases was 33. From these experiments, an empirical equation was derived:

$$U_m = \sqrt{\left(0.001 \cdot U_{10}^2 + 0.0035 h \Delta T + 0.01\right)} \quad (6)$$

where U_m is the mean air velocity in the opening (m/s); U_{10} is the mean wind speed in H = 10 m (m/s); h is the height of the opening (m); and ΔT is the temperature difference (K).

The volume flow rate (Q_v) can be found if combined with the following equation:

$$Q_v = A_{eff} \cdot U_m = \frac{1}{2} \cdot A \cdot U_m \quad (7)$$

where A_{eff} is the effective area used for inlet (m^2) and A is the total area of the window (m^2).where A_{eff} is the effective area used for the inlet (m^2) and *A* is the total area of the window (m^2). The value ½ was added because only half of the window area was used as the inlet [29].

Taking into consideration wind direction and fluctuating air movement, a series of wind tunnel experiments were conducted to determine its effect towards ventilation rate [30–32]. In 2007, Eq. (6) was revised by Larsen and Heiselberg using the tracer gas decay method [33]. By measuring different air velocities (*U*) and incident wind angles (β), a modified equation is proposed for the volume flow rate prediction:

$$Q_v = A \cdot \sqrt{C_1 \cdot f(\beta)^2 \cdot \left|C_p\right| \cdot U_{ref}^2 + C_2 \cdot \Delta T \cdot H + C_3 \cdot \frac{\Delta C_{p,opening} \cdot \Delta T}{U_{ref}^2}} \quad (8)$$

where U_{ref} is the reference wind speed and $f(\beta)$ is found by fitting a fourth order Bézier curve to the values obtained in the experiment.

Larsen and Heiselberg found values for C_1, C_2, and C_3 using the least squares method on Eq. (8), fitting it to the 159 measurements made in the wind tunnel. For parallel flow, where β=90 *or* 270°, values for the three constants were 0.0010, 0.0005 and 0.0111, respectively.

For Eqs. (6) and (8), thermal buoyancy is accepted as the dominant factor of the air change rate when wind speed is less than 1 m/s or is on the leeward side of the building [27,29,33].

3. Experimental methods

The experiments were conducted at a primary school located in a downtown area of Beijing. The primary school consisted of seven buildings, including three teaching buildings (⑤⑥ and the experiment building), two faculty offices (①③), a computer classroom building (②), and a library (④). The teaching buildings were each three stories high (Fig. 1).

The primary school selected for the experiments was a typical government-built elementary school in China. The school was surrounded by several six- and eight-story buildings on the north, west and east sides. It was shaded by 10 twenty-story buildings on the south, which blocked most of the wind and also significantly reduced the wind velocity (Fig. 2).

The selected teaching building had two symmetrical zones on the north and south (Fig. 3a). There were six standard classrooms on each floor, arranged in two rows, side by side. The two zones shared an outdoor corridor with a vitreous rain shed; as such, all classrooms had direct access to the outdoor environment (Fig. 3b).

The four selected classrooms were located on the second and third floor of the building, two facing south and the other two facing north (Fig. 4a).

The classrooms, designed to accommodate 30 students, had the following dimensions: depth = 7.65 m, width = 8.25 m, and height = 2.75 m. Each room had five plastic-steel casement

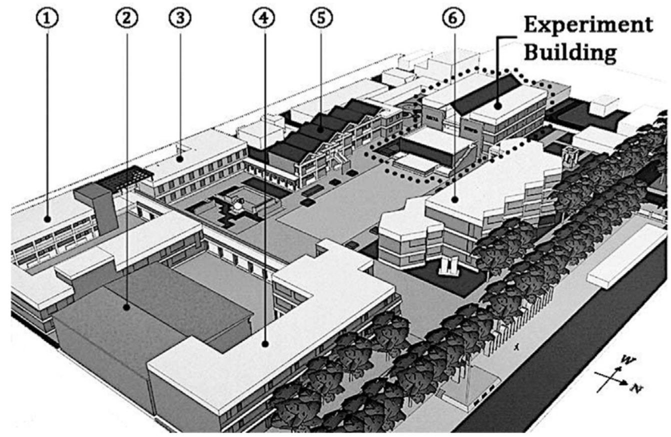

Fig. 1. Primary school layout.

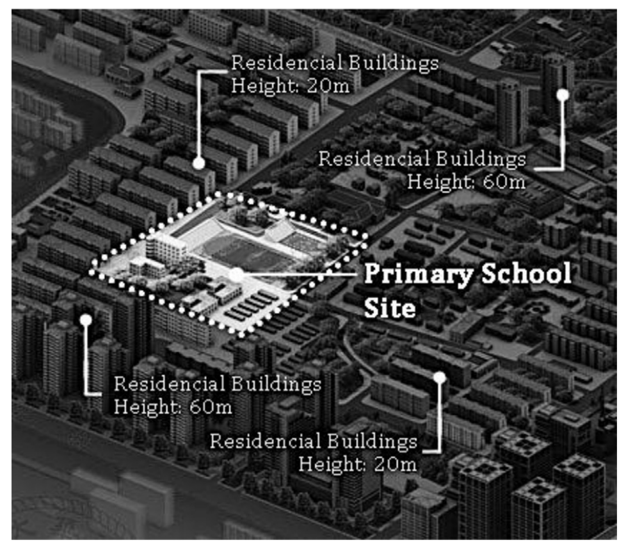

Fig. 2. School site and surroundings.

a b

Fig. 3. a: Experiment building. b: Vitreous rain shed.

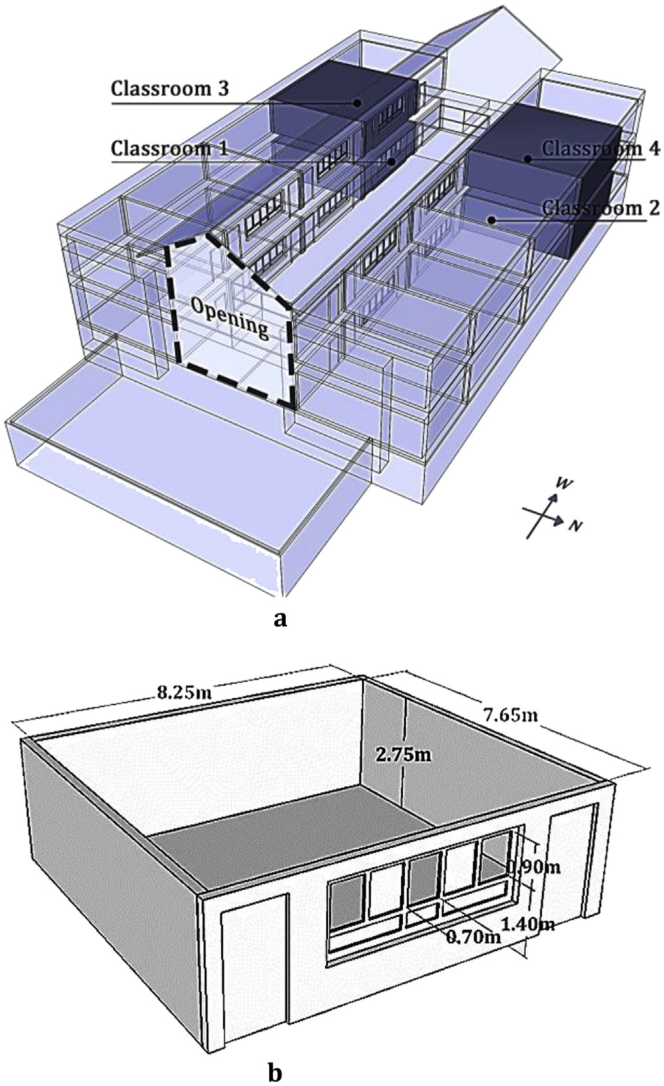

Fig. 4. a: Location of experimental classrooms. b: Dimensions of the room and window.

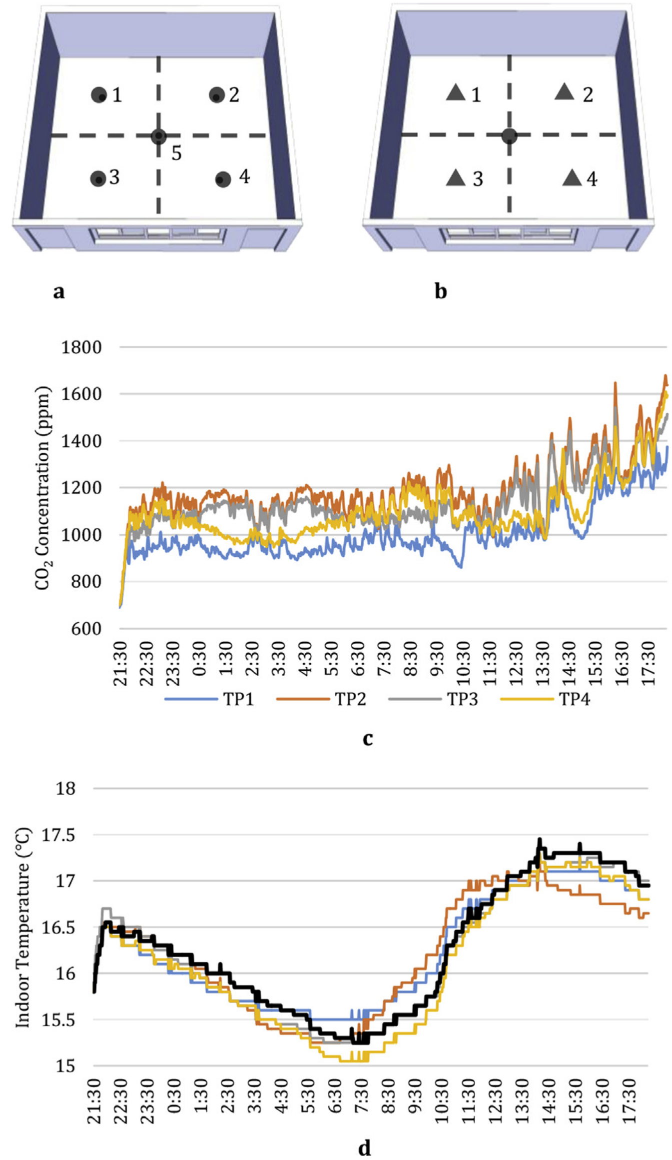

Fig. 5. a: Thermo-hygrograph Position. b: CO_2 recorder position. c: CO_2 test measurement. d: Temperature test measurement.

windows that faced the corridor, three of which could be opened. The windows had the following dimensions: height = 90 cm and width = 70 cm. The windows were completely open (>90°) during the experiments and the doors were closed (Fig. 4b).

In order to analyze the combination of buoyancy and wind effects on single-sided ventilation airflow, several experimental techniques were used. Before the formal experiments, two preliminary experiments were conducted in order to establish some of the properties (temperature and CO_2 concentration) for the latter experiments.

3.1. Preliminary experiments

For testing the uniformity of indoor temperature, five thermo-hygrographs were set in different locations of one classroom for 20 h (Fig. 5a). The thermo-hygrographs logged one sample each minute.

The results showed that all five points shared the same temperature in the deviation of ±0.2 °C, and that the thermo-hygrograph in the center of the room can adequately represent the average temperature.

For testing the air change rate of the four classrooms and the uniformity of the CO_2 concentration, the tracer gas (CO_2) decay method was applied. The concentration of CO_2 was measured by CO_2 recorders. The experiment lasted 2 h and the recorder logged one sample each minute. Four CO_2 sampling points and one thermo-hygrograph were set in each classroom (Fig. 5b). Combined with the outdoor CO_2 concentration and temperature, the calculated air change rates of the four classrooms were 1.2 h^{-1}, 1.1 h^{-1}, 1.2 h^{-1}, and 1.1 h^{-1}. This shows that the four rooms were essentially under the same ventilation conditions during the experiments. The four CO_2 recorders (in the same room) logged CO_2 concentration within a deviation of 10%, confirming the uniformity of the tracer gas in each room.

3.2. Dry ice method

A gas tracer technique with dry ice [26] was used in the experiments in order to measure the airflow rate in the room against different outdoor conditions. There was a stable release rate of the tracer gas CO_2, sublimated from dry ice in a box with a hole in its top. This method is an improvement over the constant injection method because it provides a steady and valid alternative release source for long-term ventilation rate measurements (as long as there is sufficient dry ice).

In the current experiments, three boxes of dry ice were placed in each room. During each experiment, the average indoor temperature was measured by six thermo-hygrographs placed in the center of the rooms (accuracy: ±0.1 °C). Two CO_2 recorders were simultaneously set at different locations in the rooms. One CO_2 recorder and one thermo-hygrograph were set in the outdoor corridor. Fig. 6 shows the positions of the experimental instruments. The mass of the dry ice boxes was measured at 3-h intervals during the experiments.

3.3. Measurement of environmental parameters

Wind pressure and local wind speed (U_L) were measured near the classrooms using a TSI-5825 micro manometer (accuracy: ±0.1 Pa). It was set at a location 4 m away from each classroom where the local wind velocity (U_L)was considered to have reached its maximum value in the testing zone. The height of the instrument was the same as the center of the window (Fig. 6). One sample was logged every 3 s.

A local meteorological station, located 10 m above the roof height, monitored the outdoor conditions (wind speed and direction). It logged one sample each minute.

4. Results and discussion

The driving forces of natural ventilation are temperature difference (buoyancy-driven) and wind effect. According to Chinese building codes, primary schools are generally restricted to two or three stories due to safety and egress concerns [10]. However, these schools are typically surrounded by multi-story buildings in high-density city centers. Therefore, wind speed in their vicinity is low and the temperature difference between indoor and outdoor locations is also low (in summer and season transitions). Hence, compared with buildings that have access to greater wind fields, ventilation requirements for primary schools are significantly different.

In this section, experimental results are analyzed in order to determine a dominant factor that influences airflow rate in classrooms.

The experiments were conducted for 168 h. In total, 534 valid data points were obtained from continuous measurements. One data point was calculated every 30 min. The average temperature and wind pressure were used to represent the conditions of the measured time period. The airflow rate (Q) was calculated and arranged by the temperature difference (ΔT) of the atrium and the classroom, ($\Delta T = |T_{out} - T_{in}|$) (Fig. 7).

4.1. Influential factors on airflow rate

Fig. 7 shows that $\Delta T = 1$ °C was the turning point of the tendency of Q. In order to determine the main driving force of the natural ventilation, temperature difference (buoyancy-driven), and wind effect, the data was classified by wind pressure and fitted into a linear curve. The following plots were obtained: Fig. 8a with wind pressure ≤ 0.1 Pa; Fig. 8b at 0.2 Pa; and Fig. 8c ≥ 0.3 Pa. Wind speeds were 0.0–0.3, 0.3–0.6, and 0.6–0.75 m/s, respectively.

According to the fitted curve expressions, the wind pressure exerted little influence on the airflow rate when the wind speed was less than 0.75 m/s and the temperature difference occurred between 1 and 6 °C. Thermal buoyancy was the only factor that had an effect. A significant positive correlation was found between the airflow rates and temperature difference when $\Delta T \geq 1$ °C (Fig.9). Therefore, it can be concluded that when $\Delta T \geq 1$ °C, temperature difference is the dominant factor influencing airflow rates. Finally, $\Delta T < 1$ °C was a more complicated situation; it is discussed in more detail later in the paper.

4.2. Comparison with existing correlations

Fig. 10 compares the 534 airflow rate data points measured by the gas tracer to results calculated from the first three correlations in Table 1 and to a refinement of Dascalaki's correlation. For all correlations, a discharge coefficient of 0.7 was applied (except for Dascalaki's correlation, where a coefficient of 1.0 was used [34]).

Fig. 10c shows the results calculated by Dascalaki's correction correlation in Eq. (5). Here, there was a large deviation from the measured airflow rate. The same analytical method provided in Dascalaki's paper was used to refit the parameters according to the 534 experimental data; a refined version of Dascalaki's correlation is proposed:

$$CF = 0.6187\left(Gr/Re_D^2\right)^{-0.094} \tag{9}$$

Fig. 10d was plotted based on Eq. (9); it showed considerably improved results. However, in Dascalaki's correlation, the parameters required refitting after each experiment. As such, there was

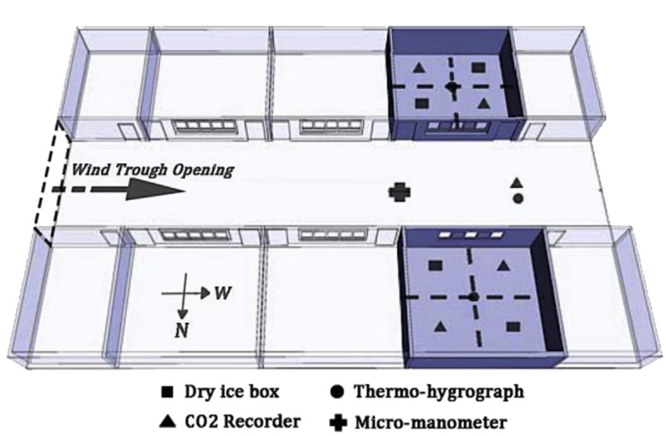

Fig. 6. Positions of experimental instruments.

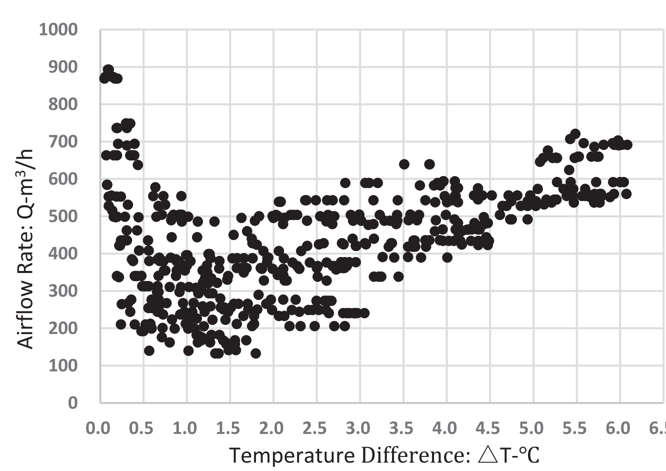

Fig. 7. Airflow rate arranged by $\Delta T = |T_{out} - T_{in}|$

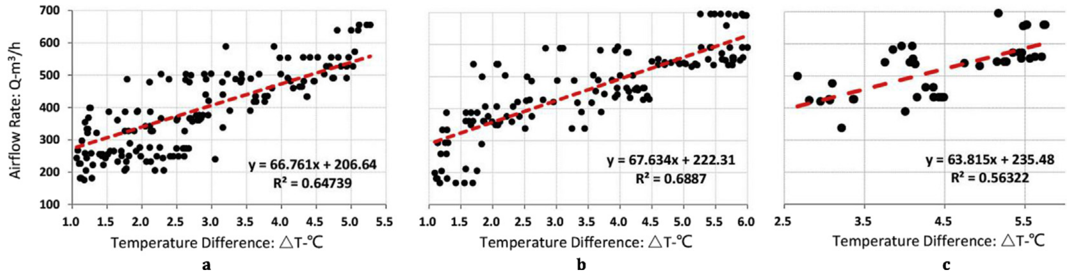

Fig. 8. a: Wind Pressure $\leq$ 0.1 Pa. b: Wind Pressure = 0.2 Pa. c: Wind Pressure $\geq$0.3 Pa.

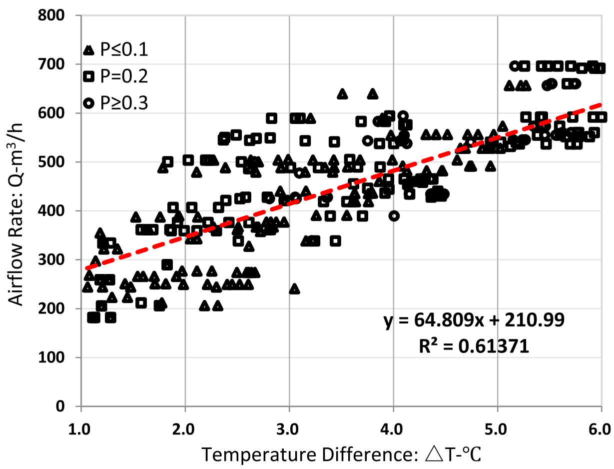

Fig. 9. Single-sided ventilation influenced by temperature difference.

not a general set of parameters that could be used for all experiments. Therefore, Dascalaki's correlation could not be used for predicting airflow rates.

In order to better compare data, the measured data points were arranged with predicted values (Fig. 11). Fig. 11 shows the amount of experimental data points that fall within the zone after setting $\pm$25% as an acceptable deviation range for each prediction. The data points located inside the dotted rectangle are points obtained when $\Delta T < 1$ °C. Table 2 summarizes the average, minimal, and maximal deviations.

The figure and table show that the predictions of airflow rates in the case of $\Delta T \geq 1$ °C were reasonably accurate for any type of correlation; however, this excluded Dascalaki's correlation, which systematically overestimated the airflow rate. Both Warren and de Gids' correlations presented a good depiction of airflow rate.

In contrast, for the case of $\Delta T < 1$ °C, the difference between measured and calculated airflow rates was large for any given correlation. The best results were obtained using de Gids and

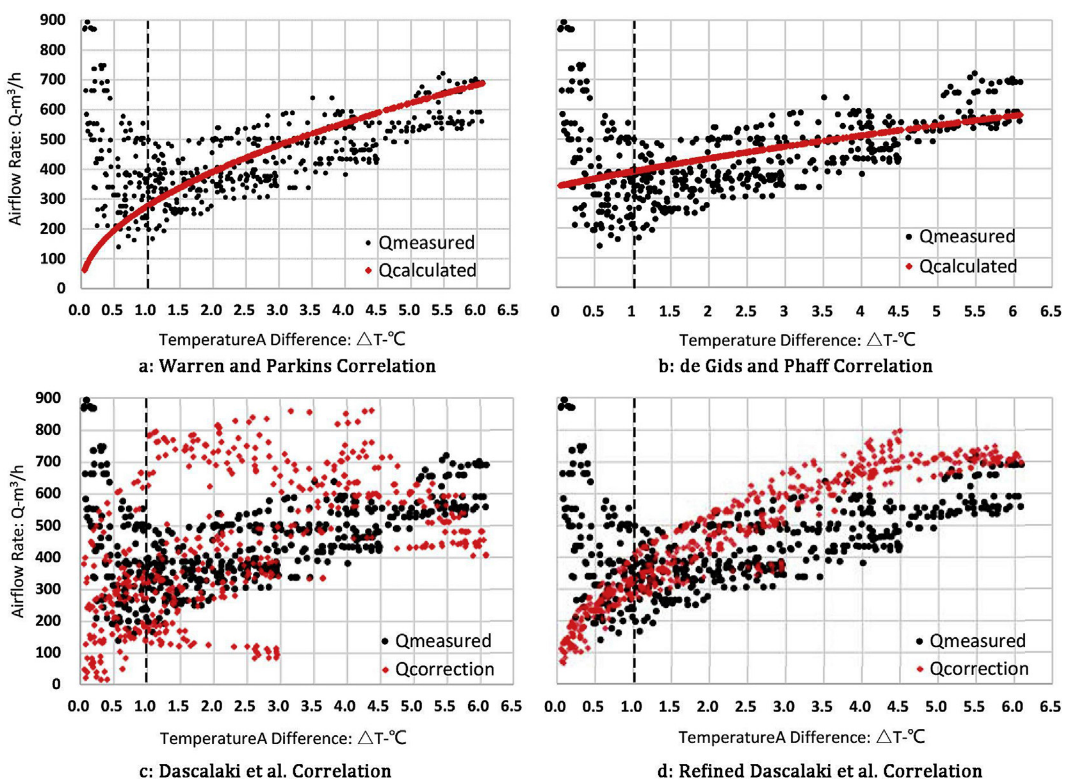

Fig. 10. Comparison among existing correlations.

Table 1
Existing correlations for calculation of airflow rate in single-sided ventilation.

Proposed by	Correlation
Warren and Parkins [27]	$Q = 1/3 \cdot C_D AgH \cdot (T_i - T_o)/T_i$
Dascalaki et al. [34]	$Q = 0.08(Gr/Re_D^2)^{-0.38} \cdot 1/3 \cdot A\sqrt{gH \cdot (T_i - T_o)/T_i}$
de Gids and Phaff [29]	$Q = 1/2 \cdot A\sqrt{(0.001 \cdot U_{10}^2 + 0.0035h\Delta T + 0.01)}$
Larsen and Heiselberg [33]	$Q = A \cdot \sqrt{C_1 \cdot f(\beta)^2 \cdot \left\|C_p\right\| \cdot U_{ref}^2 + C_2 \cdot \Delta T \cdot H + C_3 \cdot \Delta C_{p,opening} \cdot \Delta T / U_{ref}^2}$

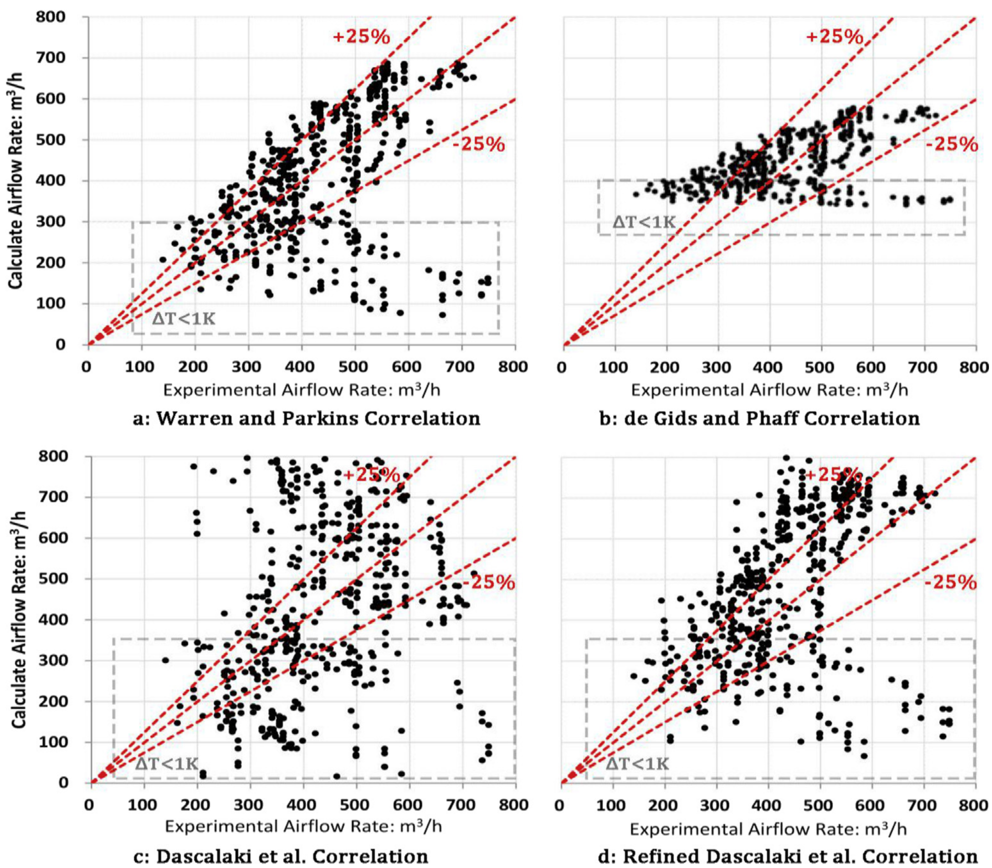

Fig. 11. Deviation analysis.

Table 2
Deviations of existing correlations.

	$\Delta T < 1$ °C			$\Delta T \geq 1$ °C			Total
	Max (%)	Min (%)	Avg.(%)	Max (%)	Min (%)	Avg.(%)	Avg.(%)
Warren and Parkins	92.91	0.42	**51.17**	72.26	0.04	**13.96**	**24.13**
De Gids and Phaff	164.53	0.02	**36.26**	135.83	0.15	**18.42**	**23.19**
Dascalaki et al.	234.41	0.80	**52.32**	301.86	0.23	**42.56**	**45.12**
Refined Dascalaki	101.76	0.77	**43.34**	132.39	0.37	**29.34**	**33.06**

Phaff's correlation, but even this correlation significantly underestimated airflow rates. Deviations up to 250% were observed using the existing correlations.

The poor performance of the existing correlations in predicting the airflow rate in the case of $\Delta T < 1$ °C was due to the fact that few experiments have previously been conducted on single-sided ventilation under the conditions of $\Delta T < 1$ °C and $U_L < 1$ m/s. Also, the decay method itself is disadvantaged because it cannot effectively obtain large quantities of data points. Due to a lack of data, the capability of the existing correlations under this condition ($\Delta T < 1$ °C) cannot be verified. Consequently, no correlation could predict the airflow rate when the indoor–outdoor temperature difference was lower than 1 °C and the wind speed was less than 1 m/s. Therefore, it is necessary to develop a new correlation that can predict airflow rates throughout the entire range of temperature differences based on the experimental data.

4.3. Evaluation of existing correlations

Previous theoretical models indicated that fluctuating air movement in an opening is one of the main sources of airflow in single-sided ventilation, especially when wind pressure and thermal buoyancy are low [29,33]. In this case, ΔP can be defined as:

$$\Delta P = P_{wind} + \Delta P_{thermal} + \Delta P_{fluct} \tag{10}$$

Using the empirical expressions P_{wind} and ΔP_{fluct} (listed in Larsen and Heiselberg's article [33]) in combination with Eq. (2), the expression of airflow rate (Q) can be adjusted to:

$$Q = C_D \cdot \frac{1}{3} A \cdot \sqrt{C_1 U_L^2 + \frac{|T_i - T_o| \cdot gH}{T_i} + \frac{C_2 \cdot |T_i - T_o|}{U_L^2}} \tag{11}$$

By fitting the 534 data samples to Eq. (11), C_1 and C_2 are now 0.01 and 0.00000053, respectively, with the correlation coefficient $R^2 = 0.099$. Under the currently proposed experimental conditions, the results calculated by Eq. (11) had little difference from Warren's correlation. This is because when $U_L < 1\ m/s$, the terms $C_1 U_L^2$ and $\frac{C_2 \cdot |T_i - T_o|}{U_L^2}$ were so small that they had little influence on the value of this equation, leaving Eq. (11) approximately the same as Eq. (2). Larsen and Heiselberg's correlation may have worked well with their experimental data, where wind velocity was larger than 1 m/s, however, this correlation was incapable of depicting circumstances where wind velocity was constantly below 1 m/s.

4.4. New hypothesis

Fig. 7 shows that 17 of the measured data points were above 600 m^3/h. Previous theories do not provide a plausible explanation for these results. Verifications confirmed that these results were not obtained by coincidence or disturbance. In order to explain this unusual deviation, the following hypothesis is proposed.

When wind pressure and thermal buoyancy are low ($U_L < 1\ m/s, \Delta T < 1°C$), then unorganized airflow in the environment may become the dominant contribution to the airflow rate. The effect here may be more significant than the correlations estimated or predicted in previous studies. When either wind pressure or thermal buoyancy rises, the unorganized airflow is repressed; therefore, airflow rates are predictable using previous correlations (such as the Bernoulli equation). Based on this unorganized airflow consideration, a new empirical correlation is proposed.

When $U_L < 1\ m/s$, $P_{wind} \ll \Delta P_{thermal}$ and $P_{wind} \ll \Delta P_{fluct}$. Therefore, the term $C_1 U_L^2$ in Eq. (11) can be disregarded. Eq. (2) works well in depicting the airflow rate (Q) when $\Delta T > 1\ °C$. The failure of Eq. (11) is due to the improper expression of ΔP_{fluct}. The key factor in the proposed correlation is to find the proper solution for the air fluctuation rate, ΔP_{fluct}.

Throughout the experiments, U_L remained less than 1 m/s and was relatively constant. However, for Eq. (11), $\Delta P_{fluct} \to \infty$ if $U_L \to 0$. Given that the desired correlation must be able to predict airflow rates for a full range of temperature differences when local wind velocity (U_L) is small, U_L now interferes in the ΔP_{fluct} depiction. Therefore, U_L is eliminated from ΔP_{fluct}.

The following correlation is now proposed:

$$Q = C_D \cdot \frac{1}{3} A \cdot \sqrt{\frac{|T_i - T_o| \cdot gH}{T_i} + \frac{C}{|T_i - T_o|}} \tag{12}$$

Fitted with the 534 data samples, the empirical constant C was found to be 0.02, with a correlation coefficient $R^2 = 0.59$. A comparison of (Q_{mea})and (Q_{cal})from Eq. (12) was plotted (Fig. 12). The discharge coefficient, C_D, was assigned 0.6 because the determination of C_D proposed by Favarolo and Manz was no longer applicable.

Compared with Table 2, the accuracy of Eq. (12) improved in both ranges of ΔT. The average deviation of Eq. (12) was reduced by 7% compared with the correlations proposed by Warren and de Gids, which were previously the best two airflow rate predictors (Table 3).

Furthermore, the newly proposed correlation can be applied across the entire range of temperature differences. When $\Delta T < 6°C$, the capability of this equation was verified by the experiments in this paper. When $\Delta T > 6°C$, the influence of the term $C/|T_i\text{-}T_o|$ became very small. Eq. (12) turned into Eq. (2) (Bernoulli equation); the capability of this equation has already been demonstrated in previous experiments and simulations.

4.5. Applicability and limitations

In summer and season transitions, Beijing (and other tier one cities in China) enjoys a meteorological situation where the mean outdoor wind velocity is below 1 m/s and the indoor–outdoor temperature difference is below 5 °C. Given that the majority of primary schools in Beijing are located in high-density urban areas, the hypothesis presented in this paper can be of great value in predicting air change rates for these schools. The hypothesis also contributes an airflow rate prediction that previous research has not been able to provide because those predictions were not valid when local wind speed was less than 1 m/s and the temperature difference was less than 1 °C. However, in the current equation, there are no parameters for wind velocity, indicating that Eq. (12) is only applicable when local wind velocity, U_L, is less than 1 m/s.

From a statistical viewpoint, the newly proposed equation suggests that the ventilation rate of a room can reach a minimal value larger than zero irrespective of how close wind velocity and temperature differences are to zero. Furthermore, experiments suggest that another factor takes control when both wind and thermal buoyancy values are close to zero. Previous studies attributed this factor to fluctuating air movement and indicated a positive correlation with temperature difference [33]. However, this paper found that there was a negative correlation between turbulence effect and temperature difference, and also that turbulence effects can become significant when temperature differences are close to zero.

Previous models and theories on natural ventilation cannot explain the findings here; as such, the validity of the newly proposed correlation in Eq. (12) still requires evaluation. Further experimental verification is also required as well as a physical model to explain the theoretical background of this equation.

5. Conclusion

This paper presented an experimental study on single-sided ventilation in primary school classrooms. The experimental results and verifications of the existing correlations showed that:

- Airflow rates were mainly influenced by thermal buoyancy when temperature differences and wind pressure were both low.
- When predicting airflow rates for $\Delta T \geq 1\ °C$, both Warren and de Gids's correlations obtained a good prediction of airflow rate within the average deviation (up to 25%).
- When predicting airflow rates for $\Delta T < 1\ °C$, the deviations of each correlation became very large and unstable because of their failure to depict air fluctuation.

Therefore, based on the experimental data, a new correlation (Eq. (12)) was proposed to predict the airflow rate for all temperature differences where the local wind velocity (U_L) was less than 1 m/s. The average deviation was reduced to 17.37%, which was 7%

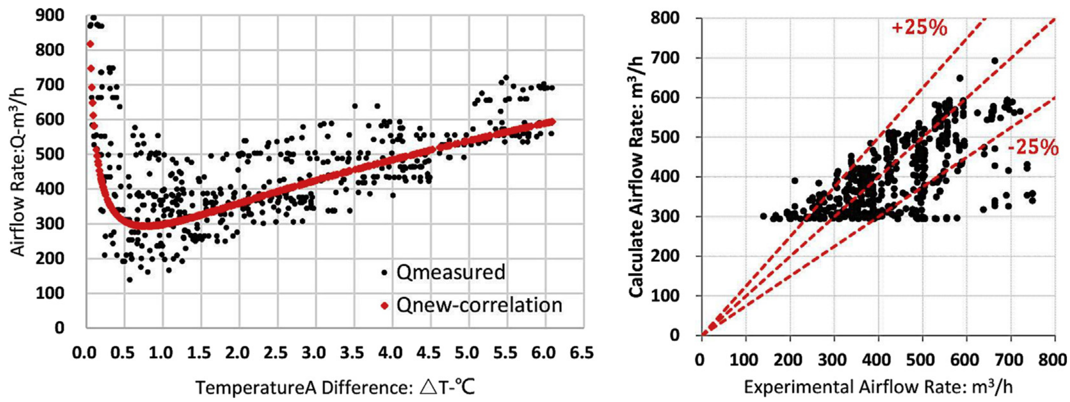

Fig. 12. Comparison of Q_{mea} and Q_{cal} of new correlation.

Table 3
Average deviation of new correlation.

	Max (%)	Min (%)	Avg.(%)
$\Delta T < 1$ °C	115.52	0.13	**28.49**
$\Delta T \geq 1$ °C	81.30	0.10	**13.60**
Total			**17.37**

less than the best existing correlations. However, the validity of this new correlation still needs to be verified. Future work should focus on verifying the proposal in this paper.

References

[1] M. Santamouris, A. Synnefa, M. Asssimakopoulos, I. Livada, K. Pavlou, M. Papaglastra, et al., Experimental investigation of the air flow and indoor carbon dioxide concentration in classrooms with intermittent natural ventilation, Energy Build. 40 (2008) 1833–1843, http://dx.doi.org/10.1016/j.enbuild.2008.04.002.

[2] R. Zhao, Y. Xia, Effective non-isothermal and intermittent air movement on human thermal responses, in: Proc. Roomvent, 1998, pp. 351–357.

[3] M.J. Finnegan, C.A. Pickering, P.S. Burge, The sick building syndrome: prevalence studies, BMJ 289 (1984) 1573–1575.

[4] J.F. Busch, A tale of two populations: thermal comfort in air-conditioned and naturally ventilated offices in Thailand, Energy Build. 18 (1992) 235–249, http://dx.doi.org/10.1016/0378-7788(92)90016-A.

[5] D.J. Clements-Croome, H.B. Awbi, Z. Bakó-Biró, N. Kochhar, M. Williams, Ventilation rates in schools, Build. Environ. 43 (2008) 362–367, http://dx.doi.org/10.1016/j.buildenv.2006.03.018.

[6] J.M. Daisey, W.J. Angell, M.G. Apte, Indoor air quality, ventilation and health symptoms in schools: an analysis of existing information, Indoor Air 13 (2003) 53–64, http://dx.doi.org/10.1034/j.1600-0668.2003.00153.x.

[7] V. Turanjanin, B. Vučićević, M. Jovanović, N. Mirkov, I. Lazović, Indoor CO2 measurements in Serbian schools and ventilation rate calculation, Energy 77 (2014) 290–296, http://dx.doi.org/10.1016/j.energy.2014.10.028.

[8] D.G. Shendell, R. Prill, W.J. Fisk, M.G. Apte, D. Blake, D. Faulkner, Associations between classroom CO2 concentrations and student attendance in Washington and Idaho, Indoor Air 14 (2004) 333–341.

[9] Code for Design of Office Buildings JGJ67-2006, Ministry of Housing and Urban-rural Construction of the People's Republic of China, 2006.

[10] Code for Design of School GB 50099—2011, Ministry of Housing and Urban-rural Construction of the People's Republic of China, 2011.

[11] Y. You, Z. Bai, C. Jia, X. Hu, W. Ran, J. Zhang, Ventilation conditions and the related symptoms in selected indoor environments in a university, in: 6th Int. Conf. Indoor Air Qual., Ventilation & Energy Conservation in Buildings IAQVEC (2007), Sendai, Japan, 2007.

[12] G.J. Levermore, The exponential limit to the cooling of buildings by natural ventilation, Build. Serv. Eng. Res. Technol. 23 (2002) 119–125.

[13] A.M. Rodrigues, A.C. da Piedade, A. Lahellec, J.Y. Grandpeix, Modelling natural convection in a heated vertical channel for room ventilation, Build. Environ. 35 (2000) 455–469.

[14] J. Hirunlabh, S. Wachirapuwadon, N. Pratinthong, J. Khedari, New configurations of a roof solar collector maximizing natural ventilation, Build. Environ. 36 (2001) 383–391.

[15] D.W. Etheridge, Unsteady flow effects due to fluctuating wind pressures in natural ventilation design—instantaneous flow rates, Build. Environ. 35 (2000) 321–337.

[16] G. Ziskind, V. Dubovsky, R. Letan, Ventilation by natural convection of a one-story building, Energy Build. 34 (2002) 91–101.

[17] P.A. Favarolo, H. Manz, Temperature-driven single-sided ventilation through a large rectangular opening, Build. Environ. 40 (2005) 689–699, http://dx.doi.org/10.1016/j.buildenv.2004.08.003.

[18] M. Caciolo, P. Stabat, D. Marchio, Numerical simulation of single-sided ventilation using RANS and LES and comparison with full-scale experiments, Build. Environ. 50 (2012) 202–213, http://dx.doi.org/10.1016/j.buildenv.2011.10.017.

[19] Y. Jiang, D. Alexander, H. Jenkins, R. Arthur, Q. Chen, Natural ventilation in buildings: measurement in a wind tunnel and numerical simulation with large-eddy simulation, J. Wind Eng. Ind. Aerodyn. 91 (2003) 331–353, http://dx.doi.org/10.1016/S0167-6105(02)00380-X.

[20] Y. Jiang, Q. Chen, Study of natural ventilation in buildings by large eddy simulation, J. Wind Eng. Ind. Aerodyn. 89 (2001) 1155–1178, http://dx.doi.org/10.1016/S0167-6105(01)00106-4.

[21] C. Allocca, Q. Chen, L.R. Glicksman, Design analysis of single-sided natural ventilation, Energy Build. 35 (2003) 785–795, http://dx.doi.org/10.1016/S0378-7788(02)00239-6.

[22] S.P. Corgnati, M. Perino, CFD application to optimise the ventilation strategy of Senate Room at Palazzo Madama in Turin (Italy), J. Cult. Herit. 14 (2013) 62–69, http://dx.doi.org/10.1016/j.culher.2012.02.007.

[23] B. Blocken, A. van der Hout, J. Dekker, O. Weiler, CFD simulation of wind flow over natural complex terrain: case study with validation by field measurements for Ria de Ferrol, Galicia, Spain, J. Wind Eng. Ind. Aerodyn. 147 (2015) 43–57.

[24] S. Gilani, H. Montazeri, B. Blocken, CFD simulation of stratified indoor environment in displacement ventilation: validation and sensitivity analysis, Build. Environ. 95 (2016) 299–313.

[25] M. Sandberg, C. Blomqvist, A quantitative estimate of the accuracy of tracer gas methods for the determination of the ventilation flow rate in buildings, Build. Environ. 20 (1985) 139–150, http://dx.doi.org/10.1016/0360-1323(85)90009-5.

[26] P.L. Cheng, X. Li, Air change rate measurements using tracer gas carbon dioxide from dry ice, Int. J. Vent. 13 (2014) 235–245, http://dx.doi.org/10.5555/2044-4044-13.3.235.

[27] P.R. Warren, L.M. Parkins, Single-sided ventilation through open windows, in: Therm. Perform. Exter. Envel. Build., ASHRAE SP 49, Florida, 1985, pp. 209–228.

[28] Y. Jiang, Q. Chen, Buoyancy-driven single-sided natural ventilation in buildings with large openings, Int. J. Heat. Mass Transf. 46 (2003) 973–988, http://dx.doi.org/10.1016/S0017-9310(02)00373-3.

[29] W. de Gids, H. Phaff, Ventilation rates and energy consumption due to open windows. A brief overview of research in the Netherlands, Air Infiltr. Rev. 4 (1982) 4–5.

[30] T. Sawachi, N. Kiyota, Y. Kodama, Airflow and wind pressure around a full-size cubical building model in a wind tunnel, in: Proc. PLEA 99 Konf. Brisbane, 1999, pp. 899–904.

[31] T. Sawachi, Detailed observation of cross ventilation and airflow through large openings by full scale building model in wind tunnel, in: Proc. ROOMVENT, 2002, pp. 565–568.

[32] Y. Tominaga, B. Blocken, Wind tunnel experiments on cross-ventilation flow of a generic building with contaminant dispersion in unsheltered and sheltered conditions, Build. Environ. 92 (2015) 452–461, http://dx.doi.org/10.1016/j.buildenv.2015.05.026.

[33] T.S. Larsen, P. Heiselberg, Single-sided natural ventilation driven by wind pressure and temperature difference, Energy Build. 40 (2008) 1031–1040, http://dx.doi.org/10.1016/j.enbuild.2006.07.012.

[34] E. Dascalaki, M. Santamouris, A. Argiriou, C. Helmis, D.N. Asimakopoulos, K. Papadopoulos, et al., Predicting single sided natural ventilation rates in buildings, Sol. Energy 55 (1995) 327–341, http://dx.doi.org/10.1016/0038-092X(95)00057-X.